

Accuracy and convergence of the backward Monte-Carlo method

Johan Carlsson¹

Oak Ridge National Laboratory, P.O. Box 2009, Oak Ridge, TN 37831-8071, USA

Abstract

The recently introduced backward Monte-Carlo method [Johan Carlsson, [arXiv:math.NA/0010118](https://arxiv.org/abs/math/0010118)] is validated, benchmarked, and compared to the conventional, forward Monte-Carlo method by analyzing the error in the Monte-Carlo solutions to a simple model equation. In particular, it is shown how the backward method reduces the statistical error in the common case where the solution is of interest in only a small part of phase space. The forward method requires binning of particles, and linear interpolation between the bins introduces an additional error. Reducing this error by decreasing the bin size increases the statistical error. The backward method is not afflicted by this conflict. Finally, it is shown how the poor time convergence can be improved for the backward method by a minor modification of the Monte-Carlo equation of motion that governs the stochastic particle trajectories. This scheme does not work for the conventional, forward method.

PACS: 02.70.Lq; 02.60.Lj

Key words: Linear parabolic partial differential equation; Monte-Carlo method; Time convergence

1 Introduction

The simplest parabolic equation is the canonical diffusion equation,

$$\frac{\partial f}{\partial t} = \frac{\partial}{\partial x} D \frac{\partial f}{\partial x}, \quad x \in \mathbb{R}, \quad 0 \leq t \leq T, \quad (1)$$

¹ E-mail: carlssonja@ornl.gov

with some initial condition $f(x, 0) = \Phi(x)$. The conventional, forward, weighted Monte-Carlo solution to Eq. (1) is given by

$$f_{\rightarrow}(x, T) = N^{-1} \sum_{i=1}^N \Phi(X_i^{\rightarrow}(0)) \times \delta(x - X_i^{\rightarrow}(T)) , \quad (2)$$

where the stochastic variables $X_i^{\rightarrow}(T)$ are found by following the stochastic trajectories given by the forward Monte-Carlo difference equation of motion:

$$X_i^{\rightarrow}(t + \Delta t) = X_i^{\rightarrow}(t) + \mu \Delta t + \zeta \sigma \sqrt{\Delta t} , \quad i = 1, \dots, N , \quad (3)$$

where $\mu = \partial D / \partial x$, $\sigma = \sqrt{2D}$, and ζ is a zero-mean, unit-variance Gaussian random number, $\zeta \in N(0, 1)$. The points where the particles are launched, $X_i^{\rightarrow}(0)$, must be chosen so that $f_{\rightarrow}(x, T=0)$, as given by Eq. (2), approximates $\Phi(x)$. The algorithm is illustrated in Fig. 1 below.

The recently introduced *backward* Monte-Carlo method [1] is both strikingly similar and fundamentally different from its older, forward sibling. The backward solution to Eq. (1) is

$$f_{\leftarrow}(x, T) = N^{-1} \sum_{i=1}^N \Phi(X_i^{\leftarrow}(0)) , \quad (4)$$

where the stochastic variables $X_i^{\leftarrow}(0)$ are found by following the stochastic trajectories given by the *backward* Monte-Carlo difference equation of motion:

$$X_i^{\leftarrow}(t - \Delta t) = X_i^{\leftarrow}(t) + \mu \Delta t + \zeta \sigma \sqrt{\Delta t} , \quad X_i^{\leftarrow}(T) = x , \quad i = 1, \dots, N . \quad (5)$$

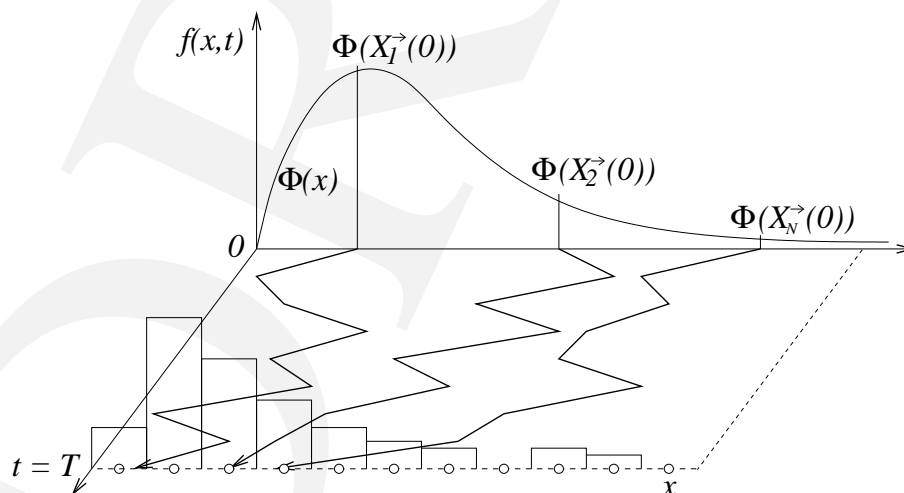


Fig. 1. The conventional, forward, weighted Monte-Carlo method. The trajectories as given by the Monte-Carlo equation of motion (3).

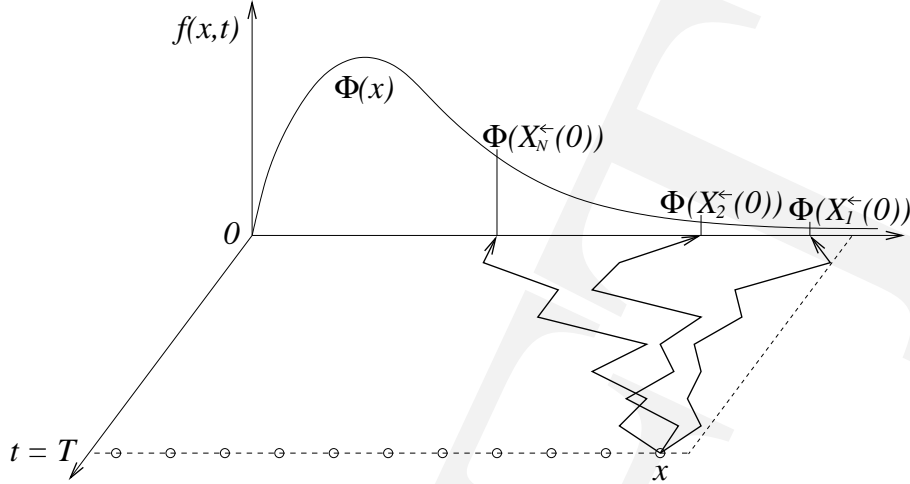


Fig. 2. The backward Monte-Carlo method. The trajectories as given by the backward Monte-Carlo equation of motion (5).

Comparing the forward and backward solutions, Eqs. (2) and (4), respectively, the appearance of δ -functions in the forward solution is the most striking difference. To understand why the backward method produces a smooth solution, i.e. without δ -functions, we have to go back to its derivation [1], which relies heavily on the Feynman-Kac formula [2]. In fact, Eq. (4), supplemented by Eq. (5), is just the numerical approximation of the stochastic Feynman-Kac representation of Eq. (1). The Feynman-Kac formula relates a parabolic equation to its *naturally associated stochastic differential equation* (SDE). This SDE governs microscopic motion going *backward* in time, and Eq. (5) is its difference approximation. As a consequence of time running in different directions in the macroscopic and microscopic world, we get the natural initial condition, $X_i^{\leftarrow}(T) = x$ in Eq. (5); i.e. we launch the particles from the point in extended phase space where we want to know the solution to the parabolic equation and let them work their way backward in time to sample from the initial condition $\Phi(X_i^{\leftarrow}(0))$ [see Fig. 2 above]. As is shown in appendix A, the forward Monte-Carlo method can be derived by forcing the naturally associated SDE to govern microscopic motion going *forward* in time. This coercion is responsible for both the δ -functions in the forward Monte-Carlo solution, Eq. (2), and the “fuzzy initial condition”, $X_i^{\rightarrow}(0) \in \{X_i^{\rightarrow}(0) \mid f_{\rightarrow}(x, T=0) \approx \Phi(x)\}$, imposed on the forward Monte-Carlo equation of motion, Eq. (3) [see appendix A for details].

However, the backward algorithm was not developed for esthetic reasons. The motivation originally came from the frustration over the extremely inefficient use of test particles of the forward method in cases where only the solution in a small part of phase space contributes significantly to the physics of interest. An example of this type of problem is the heating of fusion plasmas by cyclotron-resonance absorption on ions, where only the high-energy tail

of the solution is of relevance; but most test particles are wasted on the almost Maxwellian bulk, which has been simulated with e.g. the FIDO forward Monte-Carlo code [3]. Earlier claims [1] that the backward method is vastly superior in these cases will be substantiated in section 3.

Before that, the sources of numerical error, for both the forward and the backward method, will be identified and briefly discussed in the next section below. In section 3 we will compare the forward and backward Monte-Carlo solutions to a simple model equation. In section 4, it will be shown how a minor modification of the backward Monte-Carlo difference equation of motion, Eq. (5), leads to improved time convergence of the backward solution, Eq. (4). Finally, a summary of the main findings of this article follows in section 5.

2 Sources of error

The greatest disadvantage of the Monte-Carlo method is the unavoidable statistical error caused by the use of random numbers. With the conventional, forward Monte-Carlo method, the δ -functions in the solution [see Eq. (2)] make binning of the particles necessary. With the number of particles in each bin proportional to N/N_{bin} , the statistical error becomes $\mathcal{O}((N/N_{\text{bin}})^{-1/2})$ with obvious notations. Backing out the solution by linear interpolation between the bins introduces an error $\mathcal{O}(N_{\text{bin}}^{-2})$.

As was mentioned previously, the backward method was developed for cases where the solution is of interest only in a point or small part of phase space. In such situations it reduces the statistical error to $\mathcal{O}(N^{-1/2})$. Even in cases where the backward method is used to calculate global solutions, and the statistical error becomes $\mathcal{O}((N/N_{\text{bin}})^{-1/2})$, it does not have a finite-bin-size error because the absence of δ -functions in the solution [see Eq. (4)] makes binning superfluous.

The finite time step, Δt , also introduces an error term. An analysis of this time-step error requires some care; some mathematical subtleties are involved. There are two ways through which the time-step error can enter the numerical solution.

First, directly through the numerical approximation of the Feynman-Kac formula itself. I.e, even if we knew the *exact* stochastic variables $X_i(0)$, the backward solution, Eq. (4), would have an error due to the finite time step. To

estimate the magnitude of this error, we need to go back to the derivation of Itô's formula in Appendix A of Ref. [1] where terms of order $\mathcal{O}(\Delta t^{3/2})$ and higher were neglected. However, in the same way that the $\mathcal{O}(\Delta t^{1/2})$ -term, which was kept, becomes zero after averaging, so does the $\mathcal{O}(\Delta t^{3/2})$ -term. So, even if the $X_i^{\leftarrow}(0)$ were known to all orders, $X_i^{\leftarrow}(0) \equiv X_i(0)$, the backward solution Eq. (4), would have an error $\mathcal{O}(\Delta t^2)$. The error of the forward solution, Eq. (4) would of course be of the same order.

The other way in which the finite time step introduces an error into the solution is through an error in $X_i^{\leftarrow}(0)$. Again, going back to Ref. [1], we see that the drift term, $\mu\Delta t$, on the right-hand side of the backward Monte-Carlo equation of motion, Eq. (5), has an error $\mathcal{O}(\Delta t^{3/2})$, and the diffusive term, $\zeta\sigma\sqrt{\Delta t}$, has an error $\mathcal{O}(\Delta t)$. The different character of these two error terms should be noted; the $\mathcal{O}(\Delta t^{3/2})$ -term is deterministic whereas the $\mathcal{O}(\Delta t)$ -term is stochastic. It can be shown (see e.g. Ref. [5]) that after averaging over all the $X_i^{\leftarrow}(0)$, the approximation Eq. (5) introduces an $\mathcal{O}(\Delta t)$ error into the backward solution. Again, the situation is equivalent for the forward method.

In section 4 we will discuss how the time-step error of the backward solution can be reduced. But before that, we will study the backward and forward solutions to a simple model equation in the next section.

3 Validation and benchmarking

To validate and benchmark the backward method and to compare it to the conventional forward method, we will solve a simple model equation that has an analytic solution. We have chosen the Lorentz equation that has been used to model pitch-angle scattering in plasmas [6]:

$$\frac{\partial f}{\partial t} = \frac{\partial}{\partial x} D \frac{\partial f}{\partial x}, \quad -1 \leq x \leq 1, \quad 0 \leq t \leq T, \quad (6)$$

where the diffusion coefficient $D = (1+x)(1-x)$ and the initial condition is $f(x, 0) = \sum_{\ell=0}^{\infty} (\ell+1/2) P_{\ell}(x_0) P_{\ell}(x) e^{-\ell(\ell+1)T_0}$, where $P_{\ell}(x)$ is the Legendre polynomial. The analytic solution is $f(x, T) = \sum_{\ell=0}^{\infty} (\ell+1/2) P_{\ell}(x_0) P_{\ell}(x) e^{-\ell(\ell+1)(T_0+T)}$.

In the following we will use the parameters: $x_0 = -0.9$, $T_0 = 0.1$, and $T = 0.1$; while N , N_{bin} , and Δt will be varied so that their impact on the error can be studied. Before we get into a detailed analysis of accuracy and convergence, we show the solutions (with $N = 2 \times 10^5$, $N_{\text{bin}} = 20$, and $\Delta t = 10^{-2}$) to the Lorentz equation (6) in Fig. 3 below. Solving for $f(x, T)$ over the whole

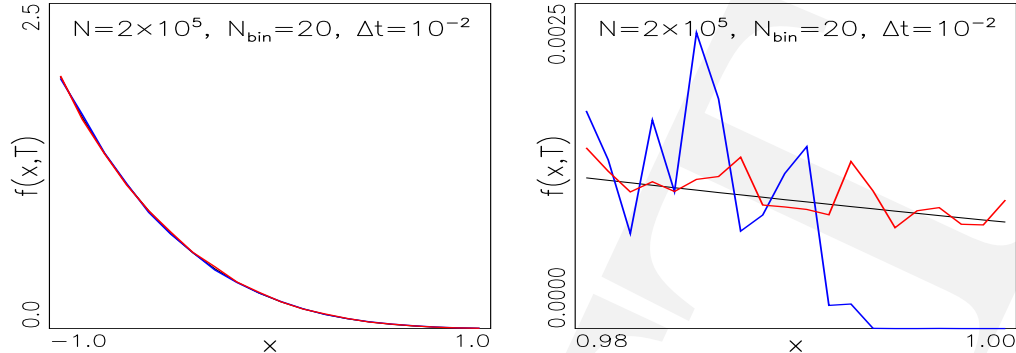


Fig. 3. Black line is analytic solution, red line is backward, and blue line is forward Monte-Carlo solution. Global solutions are to the left and tail solutions to the right.

interval $-1 \leq x \leq 1$, both the backward, $f_{\leftarrow}(x, T)$, and the forward, $f_{\rightarrow}(x, T)$ Monte-Carlo solutions are indistinguishable from the exact solution. However, solving only in the subinterval $0.98 \leq x \leq 1$, the backward solution is a much better approximation of the exact solution due to its much smaller statistical error. Note especially that the forward solution drops to zero for $x \gtrsim 0.993$ because not a single particle finds its way into the last few bins [compare also with the sketch in Fig. 1]. The ability to focus in on a small subinterval and calculate efficiently (i.e. without wasting the vast majority of the particles) the local solution is one of the main strengths of the backward Monte-Carlo method.

For a detailed error analysis we need a well-defined measure of the error. We will use the local relative error $\varepsilon_{\rightleftharpoons} = |f_{\rightleftharpoons}(x_0, T) - f(x_0, T)| / f(x_0, T)$. In the following we will plot the logarithm of the error against the logarithm of one of the parameters N , N_{bin} , and Δt , while keeping the other two parameters fixed. First we compare the statistical error of the forward and the backward solutions. To single out the statistical error from the finite bin-size and time-step errors we make the latter two small by choosing $N_{\text{bin}} = 20$, and $\Delta t = 10^{-4}$. With N spanning six decades ($N = 1, 2, 5, 10, 20, 50, \dots, 10^6$), we plot the error in the left frame of Fig. 4 below. The dotted lines are least-square fits whose slopes approximate the exponents that determine the scaling of the error. With the forward method, the bins adjacent to x_0 are empty for small N ($N = 1, 2, 20$). As a result, $\varepsilon_{\rightarrow} = 1$ for these values of N , and the slope becomes flat. The low- N data points have thus been excluded from the least-square fit to $\log \varepsilon_{\rightarrow}$. As can be seen, the statistical error [$\mathcal{O}(N^{-1/2})$ with N_{bin} fixed] then scales as predicted. The exponents -0.43 and -0.41 are as close to the theoretical value of $-1/2$ as could be expected, given the fact that the other small but non-zero error terms always tend to flatten the slope. The forward and backward methods thus converge at the same rate as N is increased, but the forward method needs N_{bin} times more particles to achieve the same accuracy as the backward method. This can easily translate into orders of magnitude in terms of execution time.

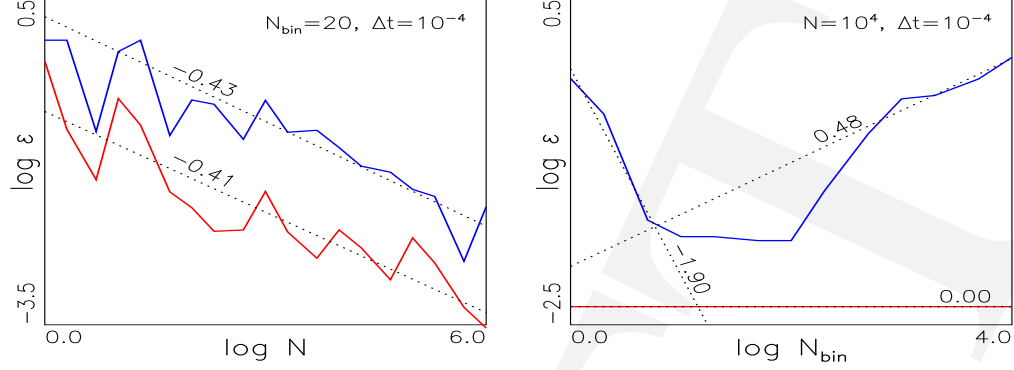


Fig. 4. Scaling of the error in the forward (blue) and backward (red) solutions. The error as a function of the number of particles (N) is plotted in the left frame, and as a function of the number of bins (N_{bin}) to the right.

Next, we study the bin-size error (and the statistical error) by varying N_{bin} over four decades ($N_{\text{bin}} = 1, 2, 5, \dots, 10^4$) while keeping fixed $N = 10^4$ and $\Delta t = 10^{-4}$. The result is shown in the right frame of Fig. 4 above. The first observation is that the backward solution is completely unaffected by the bin size; ϵ_{\leftarrow} is constant and the slope is zero. The error in the forward solution, ϵ_{\rightarrow} , exhibits a more interesting behavior with different scalings for small and large N_{bin} . With few bins there are many particles in each bin, so the statistical error is small. The bin-size error, $\mathcal{O}(N_{\text{bin}}^{-2})$, caused by backing out the solution by linear interpolation between these huge bins, however, becomes large. For small N_{bin} , the slope of $\log \epsilon_{\rightarrow}$ is -1.90, in excellent agreement with the theoretical value of -2. With many bins, the bin-size error becomes small, but with few particles in each bin, the statistical error [$\mathcal{O}(N_{\text{bin}}^{1/2})$ with N fixed] becomes dominant as is evidenced by the slope ($0.48 \lesssim 1/2$) for large N_{bin} . The shape of the $\log \epsilon_{\rightarrow}$ graph illustrates the conflict between resolution and statistics that is inherent for the forward Monte-Carlo method. The backward solution, however, can be calculated in two points arbitrarily close without affecting the statistical error. This is yet another of the main strengths of the backward method.

Turning now to the time-step error, we fix $N = 2 \times 10^5$ and $N_{\text{bin}} = 20$ and vary $\Delta t = 10^{-5}, 2 \times 10^{-5}, 5 \times 10^{-5}, \dots, 10^{-1}$. As can be seen in Fig. 5 below, both the forward and the backward methods converge as predicted (the respective slopes are $\lesssim 1$) down to a time step $\Delta t \approx 10^{-3}$. At this point the statistical error becomes dominant.

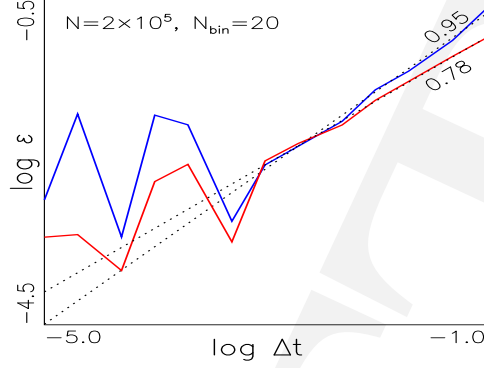


Fig. 5. The error as a function of the time step (Δt) with the forward (blue) and backward (red) methods.

4 A higher-order backward method

As was discussed in section 2, the dominant $\mathcal{O}(\Delta t)$ time-step error in the Monte-Carlo equations of motion, Eqs. (3) and (5), comes from the diffusive term $\zeta\sigma\sqrt{\Delta t}$. There is thus reason to suspect that a higher-order diffusive term might result in better overall time convergence, by reducing the time-step error to $\mathcal{O}(\Delta t^{3/2})$. In appendix B it is shown that the next-higher-order Monte-Carlo equation of motion is

$$X_i^{\vec{r}}(t \pm \Delta t) = X_i^{\vec{r}}(t) + \frac{1}{2}(1 + \zeta^2)\mu\Delta t + \zeta\sigma\sqrt{\Delta t} + \mathcal{O}(\Delta t^{3/2}). \quad (7)$$

In the left frame of Fig. 6 below the time-convergence study presented in Fig. 5 above is repeated using the higher-order approximation of Eq. (7). In the right frame exactly the same experiment is repeated with ten times more particles to further reduce the statistical error. Somewhat surprisingly, the forward solution does not converge at all. The backward solution, however, exhibits the faster time convergence we had hoped for (the slope is $\lesssim 3/2$).

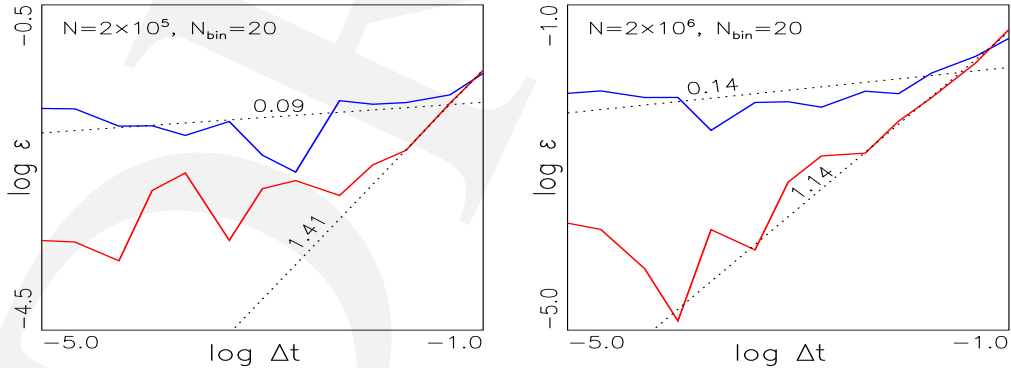


Fig. 6. The error as a function of the time step (Δt) with the higher-order forward (blue) and backward (red) methods with two hundred thousand particles (left frame) and two million particles (right frame).

Milshtein, who was not explicitly concerned with solving parabolic equations, did investigate the scaling of the error of expectation values similar to the ones of interest here [5]. His results are consistent with the $\mathcal{O}(\Delta t)$ error of the forward and backward lower-order solutions. However, for the higher-order methods introduced in this section, Milshtein's results would still indicate a $\mathcal{O}(\Delta t)$ error for both the forward and backward solutions, in clear disagreement with the scalings of Fig. 6. We hope to be able to resolve the discrepancies in future work.

5 Summary

We have shown that the backward Monte-Carlo method works as expected, i.e. it dramatically reduces the statistical error in situations where the solution is sought only in a small part of phase space. Furthermore, even in cases where we solve for the global solution, the backward method removes the conflict between resolution and statistics. This has great practical significance e.g. when the gradient of the solution is of interest.

We have also shown how a remarkably simple modification of the backward Monte-Carlo equation of motion leads to improved time convergence.

Acknowledgements

This research was sponsored by the Oak Ridge National Laboratory, managed by UT-Battelle, LLC, for the U.S. Department of Energy under contract DE-AC05-00OR22725. Research was supported in part by an appointment to the ORNL Postdoctoral Research Associates Program, administered jointly by Oak Ridge National Laboratory and the Oak Ridge Institute for Science and Education.

The author wishes to thank his colleagues in the Fusion Energy Division Radiofrequency Theory Group (Don Batchelor, Lee Berry, Mark Carter, and Fred Jaeger) for helpful comments during the work on this article.

A A new perspective on the forward Monte-Carlo method

The aim of this appendix is to derive the conventional, forward, weighted Monte-Carlo method in the same manner as the backward method was derived [1]. The starting point is the *forward* SDE:

$$dX^{\rightarrow} = \mu dt + \sigma dW . \quad (\text{A.1})$$

Solving this SDE is trivial; following exactly the same procedure as for the backward SDE, we get

$$X^{\rightarrow}(t + \Delta t) = X^{\rightarrow}(t) + \mu\Delta t + \zeta\sigma\sqrt{\Delta t} + \mathcal{O}(\Delta t) , \quad (\text{A.2})$$

where ζ is a zero-mean, unit-variance Gaussian random number, $\zeta \in N(0, 1)$. When the SDE is backward, the obvious initial condition is $X^{\leftarrow}(t=T) = x$. For the forward SDE (A.1), we simply do not know which initial condition to impose; we will have to leave $X^{\rightarrow}(t=0)$ undefined for now.

As before [1], we use the Itô formula to differentiate $f(X(t), t)$ and obtain

$$f(X^{\rightarrow}(T), T) = f(X^{\rightarrow}(0), 0) + \int_0^T 2f_t dt + \int_0^T \sigma f_x dW , \quad (\text{A.3})$$

where again we have identified $\mu = \partial D / \partial x$, $\sigma = \sqrt{2D}$, and used $f_t + \mu f_x + \frac{1}{2}\sigma^2 f_{xx} = [\text{Eq. (1)}] = 2f_t$. Using the macroscopic initial condition, $f(x, 0) = \Phi(x)$, we get

$$f(X^{\rightarrow}(T), T) = \Phi(X^{\rightarrow}(0)) - \int_0^T \sigma f_x dW . \quad (\text{A.4})$$

At this stage of the derivation of the *backward* method, we used the microscopic initial condition and found that the equivalent of the LHS of Eq. (A.4) was in fact a solution to Eq. (1): $f(X^{\leftarrow}(t=T), T) = [X^{\leftarrow}(t=T) = x] = f(x, T)$. But here, in the forward derivation, we cannot do that because $X^{\rightarrow}(T) \neq x$! Going forward in time, $X^{\rightarrow}(T)$ is an unknown; we could use the Monte-Carlo equation of motion, Eq. (A.2), to find $X^{\rightarrow}(T)$, but we do not have an initial condition! So, is there any way to get $f(x, T)$ from Eq.(A.1)? The answer is yes; there is a (rather contrived) way.

If we let $f(x, T)$ be a distribution, we can write it as

$$f(x, T) = E[f(X^{\rightarrow}(T), T) \times \delta(x - X^{\rightarrow}(T))] . \quad (\text{A.5})$$

Substituting Eq. (A.4) into Eq. (A.5), we get:

$$f(x, T) = E[\Phi(X^{\rightarrow}(0)) \times \delta(x - X^{\rightarrow}(T))] . \quad (\text{A.6})$$

The numerical approximation of this expectation value is the forward weighted Monte-Carlo solution:

$$f_{\rightarrow}(x, T) = N^{-1} \sum_{i=1}^N \Phi(X_i^{\rightarrow}(0)) \times \delta(x - X_i^{\rightarrow}(T)) . \quad (\text{A.7})$$

Now, we still need to know what the microscopic initial condition on $X_i^{\rightarrow}(0)$ should be. The best we can do is to make sure that $f_{\rightarrow}(x, T=0) \approx \Phi(x)$. Note that “approximately equal” must be given a very liberal definition because $f_{\rightarrow}(x, T=0)$ is a jagged sum of δ -functions, whereas $\Phi(x)$ is in general a smooth function. The stochastic variables $X_i^{\rightarrow}(0)$ can now be found by following the stochastic trajectories given by the forward Monte-Carlo equation of motion, Eq. (A.2), with the “fuzzy initial condition”:

$$X_i^{\rightarrow}(0) \in \{X_i^{\rightarrow}(0) \mid f_{\rightarrow}(x, T=0) \approx \Phi(x)\} . \quad (\text{A.8})$$

B A higher-order Monte-Carlo equation of motion

The diffusive term $\zeta\sigma(X(t))\sqrt{\Delta t}$ of the Monte-Carlo equations of motion, Eqs. (3) and (5), is an approximation of the Itô integral

$$\int_t^{t+\Delta t} \sigma(X(s)) dW(s) = \sigma(X(t)) \int_t^{t+\Delta t} dW(s) + \mathcal{O}(\Delta t) , \quad (\text{B.1})$$

where $X(s)$ is the stochastic process that solves the SDE

$$dX = \mu(X(s)) ds + \sigma(X(s)) dW(s) , \quad (\text{B.2})$$

where W is a Wiener process, and we impose the initial condition $X(t) = x_t$. The approximation Eq. (B.1) replaces $\sigma(x)$ with its zero-order Taylor expansion, $\sigma_0(x) = \sigma(x_t)$. To reduce the error in Eq. (5) to $\mathcal{O}(\Delta t^{3/2})$ we Taylor expand $\sigma(x)$ to first order,

$$\sigma_1(x) = \sigma(x_t) + \sigma'(x_t)(x - x_t) , \quad (\text{B.3})$$

and approximate the solution to Eq. (B.2) with

$$X(s) = x_t + \mu(x_t)(s - t) + \sigma(x_t)[W(s) - W(t)] . \quad (\text{B.4})$$

The Itô integral over σ becomes:

$$\begin{aligned}
\int_t^{t+\Delta t} \sigma(X(s)) dW(s) &= \sigma(x_t) \int_t^{t+\Delta t} dW(s) + \\
&\sigma'(x_t) \int_t^{t+\Delta t} \{\mu(x_t)(s-t) + \sigma(x_t)[W(s) - W(t)]\} dW(s) + \mathcal{O}(\Delta t^{3/2}) = \\
&\sigma(x_t) \int_t^{t+\Delta t} dW(s) + \sigma(x_t) \sigma'(x_t) \int_t^{t+\Delta t} [W(s) - W(t)] dW(s) + \mathcal{O}(\Delta t^{3/2}) ,
\end{aligned} \tag{B.5}$$

where $\mu(x_t) \int_t^{t+\Delta t} (s-t) dW(s)$ is $\mathcal{O}(\Delta t^{3/2})$ and hence was neglected. The first term on the RHS of Eq. (B.5) is just the low-order approximation Eq. (B.1). The second term is the next-order correction. To calculate this correction term, we first need some intermediate results.

Following Björk [7], we introduce the stochastic variables

$$I_n = \sum_{j=0}^{n-1} W(t_j)[W(t_{j+1}) - W(t_j)] , \tag{B.6}$$

and

$$B_n = \sum_{j=0}^{n-1} W(t_{j+1})[W(t_{j+1}) - W(t_j)] , \tag{B.7}$$

where $t_j = jt/n$, $j = 0, 1, \dots, n-1$. It trivially follows that

$$B_n + I_n = \sum_{j=0}^{n-1} [W(t_{j+1}) + W(t_j)][W(t_{j+1}) - W(t_j)] = W^2(t) , \tag{B.8}$$

and

$$B_n - I_n = \sum_{j=0}^{n-1} [W(t_{j+1}) - W(t_j)]^2 = S_n(t) . \tag{B.9}$$

In Appendix A of Ref. [1] we showed that

$$\lim_{n \rightarrow \infty} S_n(t) = t . \tag{B.10}$$

Subtracting Eq. (B.9) from Eq. (B.8) and taking the limit $n \rightarrow \infty$, we obtain

$$\lim_{n \rightarrow \infty} I_n(t) = \int_0^t W(s) dW(s) = \frac{1}{2}[W^2(t) - t] . \tag{B.11}$$

Applying Eq. (B.11) to Eq. (B.5) we get

$$\int_t^{t+\Delta t} \sigma(X(s)) dW(s) = \sigma(X(t)) [W(t+\Delta t) - W(t)] + \frac{1}{2} \sigma(X(t)) \sigma'(X(t)) \{[W(t+\Delta t) - W(t)]^2 - \Delta t\} + \mathcal{O}(\Delta t^{3/2}). \quad (\text{B.12})$$

In the absence of advection, as is the case for Eq. (1), $\sigma\sigma' = \mu$, and the higher-order Monte-Carlo equations of motion become

$$X_i^{\leftrightarrow}(t \pm \Delta t) = X_i^{\leftrightarrow}(t) + \mu\Delta t + \zeta\sigma\sqrt{\Delta t} + \frac{1}{2}(\zeta^2 - 1)\mu\Delta t + \mathcal{O}(\Delta t^{3/2}) = X_i^{\leftrightarrow}(t) + \frac{1}{2}(1 + \zeta^2)\mu\Delta t + \zeta\sigma\sqrt{\Delta t} + \mathcal{O}(\Delta t^{3/2}), \quad (\text{B.13})$$

where we have used the fact that $W(t+\Delta t) - W(t) \in N(0, \sqrt{\Delta t})$; ζ is a zero-mean, unit-variance Gaussian random number; $\zeta \in N(0, 1)$; and $\mu = \mu(X(t))$ and $\sigma = \sigma(X(t))$.

In Ref. [4] Milshtein derived Eq. (B.12) by introducing

$$X^*(t + \Delta t) = x_t + c_1\Delta t + c_2[W(t + \Delta t) - W(t)] + c_3[W(t + \Delta t) - W(t)]^2,$$

and finding the c_1 , c_2 and c_3 that minimize $E[(X^*(t + \Delta t) - X(t + \Delta t))^2]$.

References

- [1] J. Carlsson, [arXiv:math.NA/0010118](https://arxiv.org/abs/math/0010118).
- [2] Kiyosi Itô and Henry P. McKean, Jr., *Diffusion Processes and their Sample Paths*, Springer-Verlag, Berlin, 1996, ISBN: 3-540-60629-7.
- [3] J. Carlsson, T. Hellsten, and L.-G. Eriksson, in *Theory of Fusion Plasmas*, E. Sindoni, F. Troyon, and J. Vaclavik, eds., Editrice Compositori, Bologna, 1994, pp. 351–356; T. Hellsten, J. Carlsson, and L.-G. Eriksson, *Phys. Rev. Lett.* **74** (1995) 3612–3615; J. Carlsson, L.-G. Eriksson, and T. Hellsten, *Nucl. Fusion* **37** (1997) 719–723; J. Hedin, J. Carlsson, T. Hellsten, and A. Jaun, *Plasma Phys. Control. Fusion* **40** (1998) 1085–1095; J. Carlsson, T. Hellsten, and J. Hedin, *Phys. Plasmas* **5** (1998) 2885–2892; L.-G. Eriksson, M. Mantsinen, D. Borba, A. Fasoli, R. Heeter, S. Sharapov, D. F. H. Start, J. Carlsson, A. Gondhalekar, T. Hellsten, and A. Korotkov, *Phys. Rev. Lett.* **81** (1998) 1231–1234.
- [4] G. N. Milshtein, *Theory Prob. Appl.* **19** (1974) 557–562.
- [5] G. N. Milshtein, *Theory Prob. Appl.* **23** (1978) 396–401.
- [6] Allen H. Boozer and Gioietta Kuo-Petravic, *Phys. Fluids* **24** (1981) 851–859.
- [7] Tomas Björk, *Stokastisk kalkyl och kapitalmarknadsteori, Del I: Grunderna* (lecture notes), Department of Mathematics, Royal Institute of Technology, 100 44 Stockholm, Sweden.